

Near and vacuum UV polarization spectroscopy of 1,4-distyrylbenzene

Nguyen, Duy Duc; Jones, Nykola C.; Hoffmann, Søren V.; Spanget-Larsen, Jens

Published in:

Spectrochimica Acta Part A: Molecular and Biomolecular Spectroscopy

DOI:

[10.1016/j.saa.2022.122019](https://doi.org/10.1016/j.saa.2022.122019)

Publication date:

2023

Document Version

Publisher's PDF, also known as Version of record

Citation for published version (APA):

Nguyen, D. D., Jones, N. C., Hoffmann, S. V., & Spanget-Larsen, J. (2023). Near and vacuum UV polarization spectroscopy of 1,4-distyrylbenzene. *Spectrochimica Acta Part A: Molecular and Biomolecular Spectroscopy*, 286, Article 122019. Advance online publication. <https://doi.org/10.1016/j.saa.2022.122019>

General rights

Copyright and moral rights for the publications made accessible in the public portal are retained by the authors and/or other copyright owners and it is a condition of accessing publications that users recognise and abide by the legal requirements associated with these rights.

- Users may download and print one copy of any publication from the public portal for the purpose of private study or research.
- You may not further distribute the material or use it for any profit-making activity or commercial gain.
- You may freely distribute the URL identifying the publication in the public portal.

Take down policy

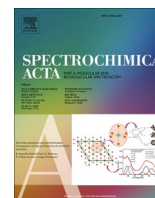
If you believe that this document breaches copyright please contact rucforsk@kb.dk providing details, and we will remove access to the work immediately and investigate your claim.



Contents lists available at ScienceDirect

Spectrochimica Acta Part A: Molecular and Biomolecular Spectroscopy

journal homepage: www.journals.elsevier.com/spectrochimica-acta-part-a-molecular-and-biomolecular-spectroscopy



Near and vacuum UV polarization spectroscopy of 1,4-distyrylbenzene

Duy Duc Nguyen^{a,1}, Nykola C. Jones^b, Søren V. Hoffmann^b, Jens Spanget-Larsen^{a,*}

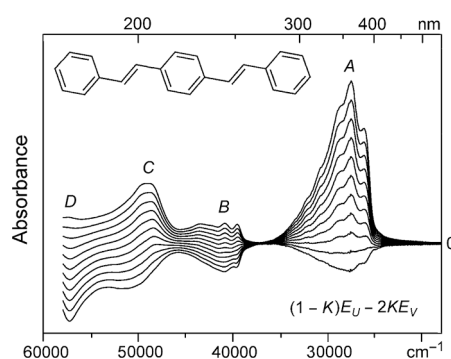
^a Department of Science and Environment, Roskilde University, Universitetsvej 1, DK-4000 Roskilde, Denmark

^b ISA, Department of Physics and Astronomy, Aarhus University, Ny Munkegade 120, DK-8000 Aarhus C, Denmark

HIGHLIGHTS

- UV absorbance of 1,4-distyrylbenzene (DSB) measured with synchrotron radiation.
- Linear Dichroism (LD) spectroscopy in the near and vacuum UV spectral regions.
- Stretched polyethylene as an anisotropic solvent.
- Semiempirical and Time-Dependent Density Functional Theory (TD-DFT) calculations.

GRAPHICAL ABSTRACT



ARTICLE INFO

Keywords:

Linear dichroism (LD)
Polarization spectroscopy
Near and vacuum UV
Synchrotron radiation
Stretched polyethylene
Time-Dependent Density Functional Theory (TD-DFT)

ABSTRACT

The UV absorbance bands of 1,4-distyrylbenzene (1,4-Bis[(*E*)-2-phenylethenyl]benzene, DSB) are investigated by Synchrotron Radiation Linear Dichroism (SRLD) spectroscopy using stretched polyethylene as an anisotropic solvent. The observed polarization data provide information on the transition moment directions of the observed spectral features. The investigation covers the range 15,000–58,000 cm⁻¹ (667–172 nm), thereby providing new information on the transitions of DSB in the vacuum UV region. The observed spectrum is characterized by four main band systems centered at 27,600, 41,000, 49,800, and 57,500 cm⁻¹ (362, 244, 201, and 174 nm). In general, the observed bands and their polarization directions are well predicted by the results of quantum chemical calculations using Time-Dependent Density Functional Theory (TD-DFT) with the functional CAM-B3LYP, and with the semiempirical all-valence-electrons method LCAO.

1. Introduction

The spectroscopic and photophysical properties of 1,4-distyrylbenzene (1,4-Bis[(*E*)-2-phenylethenyl]benzene, DSB, [Scheme 1](#)) and its derivatives have been the subject of several investigations [1–18]. DSB is

“an important prototype medium-sized π -conjugated organic compound for optoelectronics” [17] and has been characterized as “one of the working horses of optical spectroscopy” [14].

We have previously investigated the ground state absorption (GSA) spectrum of the closely related chromophore 1,4-bis(phenylethynyl)

* Corresponding author.

E-mail address: Spanget@ruc.dk (J. Spanget-Larsen).

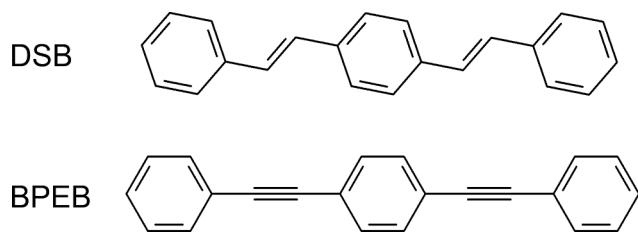
¹ Present affiliation: Duy Duc Nguyen, Intertek Vietnam Limited, Tan Binh District, Ho Chi Minh City, Vietnam.

<https://doi.org/10.1016/j.saa.2022.122019>

Received 10 September 2022; Received in revised form 12 October 2022; Accepted 17 October 2022

Available online 22 October 2022

1386-1425/© 2022 The Author(s). Published by Elsevier B.V. This is an open access article under the CC BY license (<http://creativecommons.org/licenses/by/4.0/>).



Scheme 1. 1,4-distyrylbenzene (DSB) and 1,4-bis(phenylethynyl)benzene (BPEB).

benzene (BPEB, [Scheme 1](#)) [19]. In the present publication, we report the results of a similar study of DSB. The absorbance spectrum is investigated by UV Synchrotron Radiation Linear Dichroism (SRLD) spectroscopy on partially aligned molecular samples using stretched polyethylene (PE) as an anisotropic solvent. LD polarization spectroscopy on oriented molecular assemblies yields information on the polarization directions of the recorded absorption bands [20–25], information that frequently leads to resolution of otherwise overlapping spectral features. The use of synchrotron radiation [19,26,27] allows extension of the measurements up to about $58,000\text{ cm}^{-1}$ (172 nm), thereby providing evidence for previously unobserved transitions of DSB in the vacuum UV region. The observed spectral features are compared with theoretical electronic transitions computed with the semiempirical all-valence-electrons models ZINDO [28,29] and LCOAO [30,31] and with Time-Dependent Density Functional Theory (TD-DFT) [32–35] using the functionals LC- ω PBE [36,37], ω B97XD [38], and CAM-B3LYP [39]. For previous theoretical calculations of the electronic transitions of DSB, see literature referenced by Roldao et al. [17]. Additional information is provided as [Supplementary data](#), referred to in the ensuing text as S1–S6.

2. Experimental

2.1. Sample preparation

1,4-distyrylbenzene (DSB) [CAS 1608–41-9] (>95 %) was purchased from ChemDiv Inc. The spectroscopic purity of the substance was checked by comparison with literature spectra [4,6,17,40,41]. Low-density polyethylene (PE) was obtained as pure 100 μm sheet material from Hinnum Plast, Denmark. DSB was introduced into the PE by submersion of a piece of the polymer sheet into a saturated solution of the compound in chloroform (Merck Uvasol) at 50 $^{\circ}\text{C}$ for a week. To accelerate the process, the solution was sonicated in an ultrasound bath for thirty minutes each day. Subsequently, the chloroform was allowed to evaporate from the doped sample and crystalline deposits on the surface were removed with methanol (Merck Uvasol). The sheet sample was finally uniaxially stretched by ca. 500 %. A reference sample without solute was produced in the same manner. Further details on stretched PE samples can be found in the literature [20–25].

2.2. Linear Dichroism (LD) spectroscopy

Two linearly independent absorbance curves were measured at room temperature, one with the electric vector of the sample beam parallel to the uniaxial stretching direction (U), and one with the electric vector perpendicular to it (V); in both cases the sample beam was perpendicular to the surface of the PE sheet. The resulting baseline-corrected LD absorbance curves $E_U(\bar{\nu})$ and $E_V(\bar{\nu})$ are shown in [Fig. 1](#) (top).

The $15,000\text{--}47,000\text{ cm}^{-1}$ (667–213 nm) region was recorded using a Shimadzu UV-2101PC spectrophotometer equipped with rotatable Glan-Taylor prism polarizers in sample and reference beams. The instrument was validated by an internal calibration procedure. The $37,000\text{--}58,000\text{ cm}^{-1}$ (270–172 nm) region was measured with synchrotron radiation as previously described [19] on the CD1 beamline [26,27] at the storage

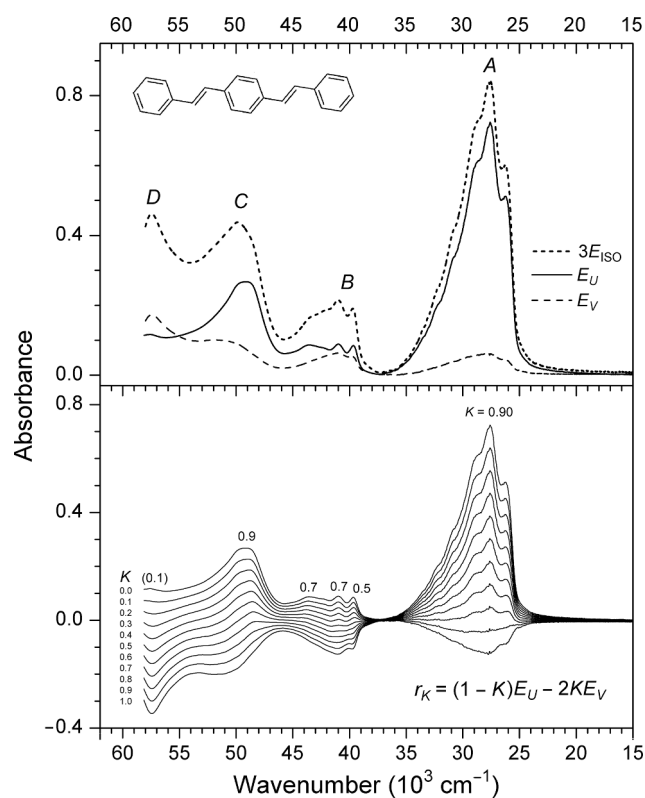


Fig. 1. Top: Linear Dichroism (LD) absorbance curves $E_U(\bar{\nu})$ and $E_V(\bar{\nu})$ for 1,4-distyrylbenzene (DSB) in stretched polyethylene measured at room temperature with the electric vector of the sample beam parallel and perpendicular to the uniaxial stretching direction U . $3E_{\text{ISO}}(\bar{\nu}) = E_U(\bar{\nu}) + 2E_V(\bar{\nu})$ is three times the absorbance that would have been measured in an isotropic experiment on the same sample. Bottom: Family of reduced absorbance curves $r_K(\bar{\nu}) = (1 - K)E_U(\bar{\nu}) - 2KE_V(\bar{\nu})$ with K varying from 0 to 1 in steps of 0.1.

ring ASTRID at the Centre for Storage Ring Facilities (ISA). The same physical sample was used in both experiments; combination of the two data sources was unproblematic. Validation was undertaken by checking the overlap region of the two recorded spectra.

3. Computational details

Quantum chemical calculations of the electronic transitions of DSB were carried out with the semiempirical all-valence-electrons models ZINDO [28,29] and LCOAO [30,31], and with TD-DFT procedures adopting the long range-corrected density functionals LC- ω PBE [36,37], ω B97XD [38], and CAM-B3LYP [39]. The ZINDO and the TD-DFT calculations were performed with the Gaussian 16 software package [42], the LCOAO calculation with the computer program published in Ref. [43].

The TD-DFT calculations considered vertical transitions from the electronic ground state to the 110 lowest excited singlet states, using the basis set AUG-cc-pVTZ [44,45]. The ground state molecular equilibrium geometries were optimized with the respective functionals under the assumption of C_{2h} symmetry. In the optimizations performed with LC- ω PBE and CAM-B3LYP, dispersion effects were represented by the model by Grimme [46], empirical dispersion = gd3bj [42] (the ω B97XD functional includes empirical dispersion [38]). In all the DFT and TD-DFT calculations, the influence of the solvent medium was approximated by the Polarizable Continuum Model IEFPCM [47–50] using solvent = n -hexadecane [42]. The C_{2h} equilibrium coordinates predicted with CAM-B3LYP/AUG-cc-pVTZ are given in S1. One very small imaginary torsional frequency equal to $i2.4\text{ cm}^{-1}$ is predicted (S1), indicating that the assumption of planarity is acceptable. A selection of electronic

transitions predicted with TD-CAM-B3LYP is listed in Table 1, complete results are provided in S2.

The calculations performed with the ZINDO method considered excitations to the 110 lowest excited singlet states [42]. The LCOAO calculation included interaction between all singlet configurations generated by promotion of an electron from the 11 highest occupied to the 11 lowest unoccupied π -type molecular orbitals (MOs). The LCOAO calculation provided prediction of MCD B-terms [20,31,51] for the computed transitions. The C_{2h} molecular input geometry for the ZINDO and LCOAO calculations was taken as the one predicted with B3LYP [52,53] using the basis set cc-pVTZ [44,45]. The LCOAO results are provided as S3 and S4 (a complete LCOAO bibliography is included as S5).

A graphical comparison of the electronic transitions predicted with ZINDO, LCOAO, TD-LC- ω PBE, TD- ω B97XD, and TD-CAM-B3LYP is shown in Fig. 2. The convolutions of the predicted transitions were performed by assigning a Gaussian function to each excitation wavenumber with an area proportional to the oscillator strength of that transition, using a constant standard deviation, $\sigma = 1500 \text{ cm}^{-1}$. The molecular orbital (MO) surface diagrams shown in Fig. 3 were computed with CAM-B3LYP/AUG-cc-pVTZ and visualized using GaussView 6 [54] with a constant isovalue equal to 0.02.

4. Results and discussion

4.1. Linear dichroism: orientation factors and polarization directions

The observed LD absorption curves $E_U(\tilde{\nu})$ and $E_V(\tilde{\nu})$ are shown in Fig. 1 (top). The investigated spectral range is characterized by four main band systems: A, B, C, and D centered at 27,600, 41,000, 49,800, and around 57,500 cm^{-1} (362, 244, 201, and 174 nm) (Table 1); the energy position of the latter band is quoted with less accuracy, due to its close proximity to the spectrophotometers low-wavelength cut-off. The

directional information that can be obtained from the LD curves is represented by the orientation factors K_i for the transition dipole moments of the observed transitions [20–24]:

$$K_i = \langle \cos^2(M_i, U) \rangle \quad (1)$$

Here (M_i, U) is the angle of the moment vector M_i of transition i with the stretching direction U of the polymer. The pointed brackets indicate the average over all solute molecules in the light path. A large K_i indicates that the transition moment is efficiently aligned with the stretching direction, and vice versa. The K_i values may be determined by the graphical TEM (Trial and Error Method) procedure [20–22]. We consider the reduced absorbance curves $r_K(\tilde{\nu})$ [22]:

$$r_K(\tilde{\nu}) = (1 - K)E_U(\tilde{\nu}) - 2KE_V(\tilde{\nu}) \quad (2)$$

The contribution from transition i vanishes from the linear combination $r_K(\tilde{\nu})$ for $K = K_i$. Provided a spectral feature due to transition i can be identified in both $E_U(\tilde{\nu})$ and $E_V(\tilde{\nu})$, the K_i value may thus be determined by visual inspection [22]. A family of curves $r_K(\tilde{\nu})$ for DSB with K ranging between the limits 0 and 1 is shown in Fig. 1 (bottom). The estimated orientation factors K for the observed spectral features are listed in Table 1.

A well-defined K value equal to 0.90 is determined for the strong band A peaking at 27,600 cm^{-1} (362 nm). The large value indicates that the moment vector is well aligned with the stretching direction. An even larger K equal to 0.95 was determined for the corresponding transition in the spectrum of BPEB [19].

Band B displays three closely spaced peaks at 39,700, 41,000, and 43,700 cm^{-1} (252, 244, and 229 nm) with smaller K values close to 0.5, 0.7, and ~ 0.7 . The value for the latter peak is approximate because of the broadness of this feature. A close-up of the family of reduced absorbance curves for band B is provided in S6.

The bands C and D in the vacuum UV region with maxima near 49,800 and 57,500 cm^{-1} (201 and 174 nm) are relatively broad and

Table 1

Observed spectral features and calculated electronic transitions for 1,4-distyrylbenzene (DSB).

Experimental	$\tilde{\nu}^a$	$3E_{\text{ISO}}^b$	K^c	$ \phi ^d$	TD-CAM-B3LYP/AUG-cc-pVTZ				Leading configurations ^g
					Term ^e	$\tilde{\nu}^a$	f^f	ϕ^d	
A	27.6	0.85	0.90	(0°)	1 ¹ B _u	27.8	1.95	(0°)	93 % [6b _g → 6a _u], 5 % [5a _u → 7b _g]
					2 ¹ A _g	36.0	0	–	49 % [6b _g → 7b _g], 44 % [5a _u → 6a _u]
					2 ¹ B _u	37.4	0.06	+5°	40 % [6b _g → 7a _u], 33 % [4b _g → 6a _u]
					3 ¹ B _u	39.6	0.01	+23°	23 % [6b _g → 8a _u], 21 % [5b _g → 6a _u]
					3 ¹ A _g	39.8	0	–	28 % [6b _g → 8b _g], 23 % [4a _u → 6a _u]
B	39.7 41.0 43.7	0.19 0.22 0.17	0.5 0.7 0.7	43° 29° 29°	4 ¹ A _g	41.3	0	–	43 % [6b _g → 7b _g], 41 % [5a _u → 6a _u]
					1 ¹ B _g	41.8	0	–	68 % [6b _g → 33a _g], 16 % [6b _g → 34a _g]
					4 ¹ B _u	43.4	0.30	+24°	40 % [4b _g → 6a _u], 14 % [6b _g → 7a _u]
					5 ¹ B _u	44.4	0.28	+61°	19 % [5b _g → 6a _u], 22 % [6b _g → 9a _u]
					6 ¹ B _u	46.3	0.18	+45°	29 % [6b _g → 9a _u], 25 % [5b _g → 6a _u]
C	49.8	0.44	(0.9)	(0°)	7 ¹ B _u	47.5	0.01	+27°	50 % [3b _g → 6a _u], 23 % [6b _g → 9a _u]
					8 ¹ B _u	50.9	0.24	–8°	15 % [5a _u → 7b _g], 15 % [6b _g → 10a _u]
					9 ¹ B _u	51.8	0.87	–7°	19 % [4b _g → 7a _u], 13 % [6b _g → 10a _u]
					10 ¹ B _u	52.9	0.02	–5°	33 % [5a _u → 7b _g], 22 % [6b _g → 10a _u]
					11 ¹ B _u	54.4	0.01	–71°	18 % [5b _g → 6a _u], 12 % [5a _u → 8b _g]
D	(57.5)	0.47	(0.1)	(76°)	12 ¹ B _u	54.6	0.06	–29°	19 % [6b _g → 10a _u], 17 % [4b _g → 7a _u]
					13 ¹ B _u	55.1	0.01	–79°	58 % [6b _g → 11a _u], 12 % [5a _u → 9b _g]
					14 ¹ B _u	57.0	0.40	+58°	29 % [5a _u → 8b _g], 21 % [4a _u → 7b _g]
					15 ¹ B _u	58.0	0.22	–74°	55 % [6b _g → 12a _u], 12 % [5a _u → 10b _g]
					16 ¹ B _u	59.9	0.06	+50°	59 % [4b _g → 9a _u], 11 % [4b _g → 8a _u]
					17 ¹ B _u	60.5	0.38	–64°	49 % [2b _g → 6a _u], 13 % [3a _u → 7b _g]
					18 ¹ B _u	61.5	0.10	+79°	37 % [3b _g → 7a _u], 16 % [3b _g → 8a _u]
19 ¹ B _u	61.7	0.11	–73°	15 % [4a _u → 9b _g], 10 % [6b _g → 13a _u]					
20 ¹ B _u	62.3	0.00	+19°	22 % [6b _g → 13a _u], 15 % [4a _u → 9b _g]					

^a Peak wavenumber in 1000 cm^{-1} .

^b $3E_{\text{ISO}} = E_U + 2E_V$ (Fig. 1, top).

^c Orientation factor (Section 4.1).

^d In-plane transition moment angle (Scheme 2).

^e Selected terms. Full listing provided as S2.

^f Oscillator strength.

^g Some important MOs are shown in Fig. 3.

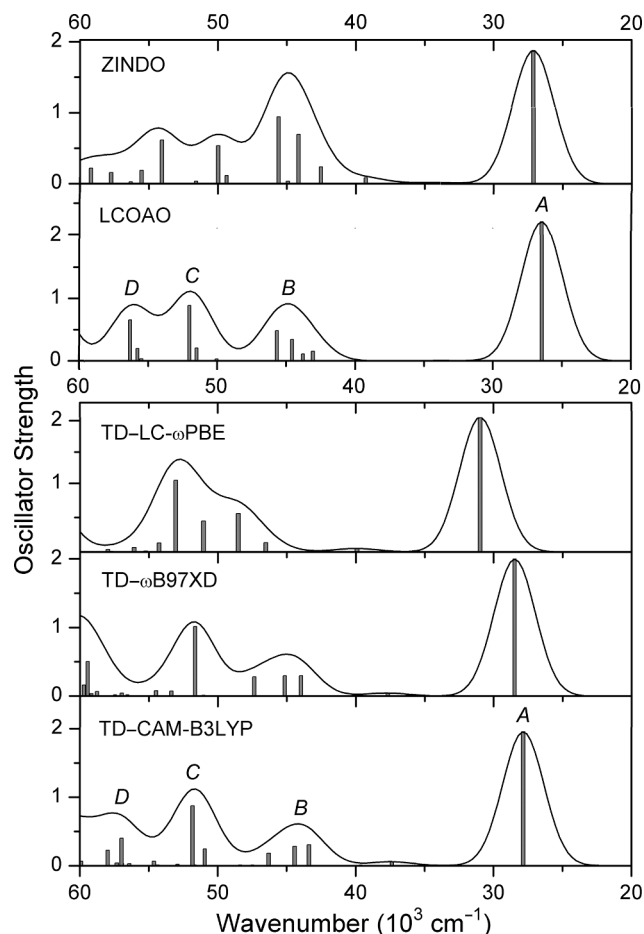


Fig. 2. Gaussian convolutions of electronic transitions for 1,4-distyrylbenzene (DSB) predicted with the semiempirical all-valence-electrons methods ZINDO and LCOAO, and with TD-DFT procedures using the functionals LC- ω PBE, ω B97XD, and CAM-B3LYP.

featureless. The absorption in this spectral region is likely to contain overlapping contributions from several electronic transitions. K s around 0.9 and 0.1 are estimated for the two maxima. These values are necessarily approximate, but they clearly indicate that the bands C and D are dominated by differently polarized contributions.

Further analysis of the LD data is complicated by the low molecular symmetry of DSB. We shall assume that the observed absorption is primarily due to π - π^* transitions and thus polarized in the molecular plane (this assumption is supported by the calculated results (S2)). But according to the C_{2h} molecular point group, infinite moment directions are possible for in-plane polarized transitions. We thus need to determine the angles ϕ_i formed by the moments of the observed transitions i with a specific, well-defined axis in the plane. This axis is usually chosen as the “orientation axis” [20,21], that is the molecular axis y corresponding to the largest value of the average cosine squared, $\langle \cos^2(y, U) \rangle = K_y$, also called the “long axis” of the molecule. The in-plane “short axis” x perpendicular to y corresponds to the lowest average cosine squared among directions in the plane, $\langle \cos^2(x, U) \rangle = K_x$ [20,21]. The C_2 symmetry axis z is perpendicular to x and y , and we have $K_x + K_y + K_z = 1$. For a transition i polarized in the molecular x, y plane, the following relation holds [20]:

$$|\phi_i| = \tan^{-1} \sqrt{(K_y - K_i)/(K_i - K_x)} \quad (3)$$

Provided the orientation factors K_x and K_y for the in-plane axes x and y can be derived, the numerical values of the individual transition moment angles ϕ_i can thus be estimated from the observed K_i values. In

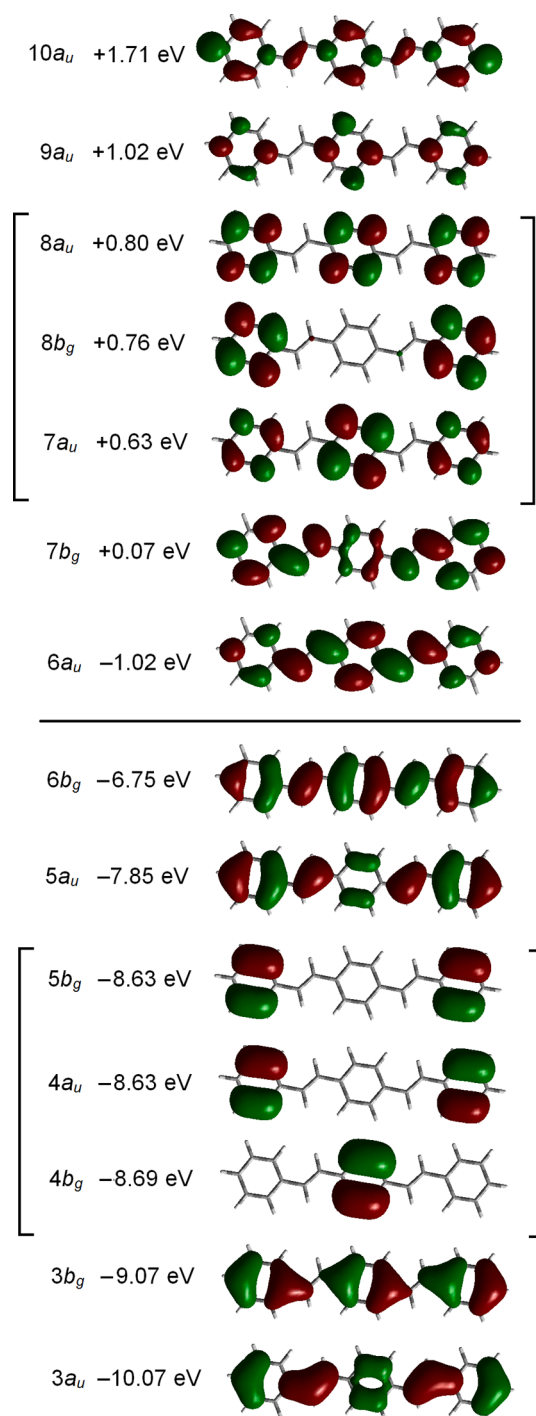
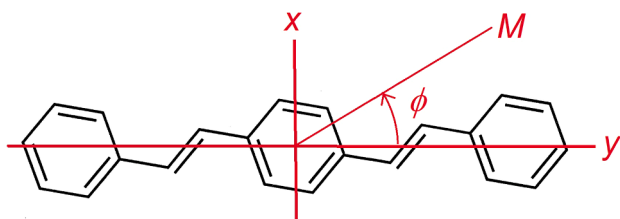


Fig. 3. Surface diagrams of the seven highest occupied and seven lowest unoccupied π -type MOs for 1,4-distyrylbenzene (DSB) computed with CAM-B3LYP/AUG-cc-pVTZ with indication of symmetries and energies.

view of the highly elongated molecular shape of DSB we shall assume that the orientation in stretched PE is rod-like [20], $K_y \gg K_x = K_z$, with orientation axis y corresponding to the longest molecular dimension (see Scheme 2). According to the calculated results (see below), the transition responsible for the intense band A is polarized along this axis (S2), and we shall thus adopt the value $K_y = K_A = 0.90$ (the corresponding Saupe orientation parameter [23,24] is $S = (3K - 1)/2 = 0.85$). The absolute moment angles $|\phi_i|$ derived from Eqn. (3) with $K_y = 0.90$ and $K_x = (1 - K_y)/2 = 0.05$ are listed in Table 1.



Scheme 2. Definition of in-plane transition moment angle ϕ (see text).

4.2. Electronic transitions

Roldao et al. [17] have recently compared the electronic transitions of DSB obtained with several advanced theoretical procedures, including CASPT2//CASSCF, considering the near UV region up to about $40,000\text{ cm}^{-1}$ (250 nm). The orbital structure of DSB is characterized by near-degeneracies of π and π^* MOs in the regions next to the frontier region (Fig. 3, S2, S3), just as in the case of BPEB [19] which is *iso*- π -electronic with DSB. The predicted states in the high-wavenumber range thus tend to be of a composite nature, with essentially first order interactions between several near-degenerate electronic configurations, and the computed transitions are likely to be sensitive to calculational details. The transitions obtained with the present collection of semi-empirical and TD-DFT theoretical procedures are compared in Fig. 2 covering the region up to $60,000\text{ cm}^{-1}$ (167 nm). The overall structure of the observed spectrum with four main band systems A, B, C, and D (Fig. 1) is not well-reproduced by the TD-LC- ω PBE calculation, and ZINDO fails to predict the observed intensity distribution. The TD- ω B97XD and TD-CAMB3LYP results are quite similar, particularly in the regions of band A and B. We shall base our discussion on the TD-CAM-B3LYP (Table 1, S2) and LCOAO (S3, S4) results which are mutually consistent (Fig. 2) and in agreement with the observed general band structure throughout the investigated range.

The intense band A has an onset at $26,200\text{ cm}^{-1}$ (382 nm) and a maximum at $27,600\text{ cm}^{-1}$ (362 nm). Relative to spectra of DSB in liquid solution [4,6,17,40,41], the resolution of the vibrational fine structure of band A is improved in the present spectrum. This can probably be explained by the planarization effect of the stretched PE medium [19,55–57], reducing the torsional mobility of the solute molecule. Band A must be assigned to the 1^1B_u state predicted at $27,800\text{ cm}^{-1}$ (360 nm). This state is well described by the HOMO-LUMO excitation, $6b_g(\pi) \rightarrow 6a_u(\pi^*)$ (see Fig. 3) and is predicted to be polarized along the long axis y (for details, see S2). The corresponding long axis-polarized band in the spectrum of BPEB (Scheme 1) was observed at $28,900\text{ cm}^{-1}$ (346 nm) [19].

Several transitions are predicted in the region between bands A and B (Table 1), but they are not clearly observed in the present investigation. Transitions to the optically allowed states 2^1B_u and 3^1B_u computed at $37,400$ and $39,600\text{ cm}^{-1}$ (267 and 253 nm) are weak. They are essentially long axis-polarized and are likely to be buried under the tail of the strong, long axis-polarized band A. In the case of BPEB (Scheme 1) with D_{2h} molecular symmetry, transitions to the corresponding states 1^1B_{2u} and 2^1B_{2u} are short axis-polarized and a weak feature at $37,400\text{ cm}^{-1}$ (267 nm) in the LD spectrum of BPEB was assigned to these transitions [19]. Based on an analysis of the fluorescence emission and excitation spectra of DSB, Gierschner et al. [4,5] estimated a wavenumber around $33,000\text{ cm}^{-1}$ (300 nm) for the 2^1B_u state. The state may possibly be observed directly by MCD spectroscopy, LCOAO predicts a positive MCD B-term for 1^1B_u but a negative B-term for 2^1B_u computed at $33,600\text{ cm}^{-1}$ (298 nm) with this method (S3, S4).

The states 2^1A_g , 3^1A_g , and 4^1A_g of DSB calculated at $36,000$, $39,800$, and $41,300\text{ cm}^{-1}$ (278, 251, and 242 nm) are electronically forbidden, but they may borrow long axis-polarized intensity by vibronic coupling with the strong band A via b_u symmetric molecular vibrations. The 1^1A_g states are of particular interest in excited state absorption (ESA)

spectroscopy; a strong feature at 1.67 eV ($13,500\text{ cm}^{-1}$) in the ESA spectrum of DSB was thus assigned to the transition $1^1B_u \rightarrow 3^1A_g$ by Oliveira et al. [14] (see also [17]).

Band B displays three closely spaced features at $39,700$, $41,000$, and $43,700\text{ cm}^{-1}$ (252, 244, and 229 nm). This absorption band is most likely due to the electronic states 4^1B_u , 5^1B_u , and 6^1B_u predicted at $43,400$, $44,400$, and $46,300\text{ cm}^{-1}$ (230, 225, and 216 nm) (Table 1), but the strong overlap between the observed features prevents a more detailed assignment. The estimated experimental moment angles $|\phi|$ (Table 1) indicate directions in the intermediate range between short and long axis polarization, consistent with the fluorescence anisotropy reported for a tetra-*t*-butyl derivative of DSB [3]. The theoretically predicted moment angles $+24^\circ$, $+61^\circ$, and $+45^\circ$ (Table 1) are in qualitative agreement with the experimental estimate. Strong MCD B-terms with alternating signs are predicted in the region of band B (S3, S4), an analysis of the MCD spectrum may be rewarding.

The high wavenumber region is dominated by two strong bands C and D with maxima near $49,800$ and $57,500\text{ cm}^{-1}$ (201 and 174 nm) and absolute moment angles $|\phi|$ close to 0° and 76° (Table 1). The estimated angles are approximate (Section 4.1), but they clearly indicate that the bands C and D are predominantly long and short axis-polarized, respectively. The theoretical prediction of the numerous electronic states expected in this region is difficult, and the results of the present calculations must be considered as preliminary. We tentatively assign band C to the states 8^1B_u and 9^1B_u predicted at $50,900$ and $51,800\text{ cm}^{-1}$ (196 and 193 nm) with moment angles ϕ equal to -8° and -7° (Table 1). A number of states are predicted to contribute to band D, primarily 14^1B_u and 15^1B_u at $57,000$ and $58,000\text{ cm}^{-1}$ (175 and 172 nm) with ϕ equal to $+58^\circ$ and -74° , but several additional states are likely to be involved. Within the limits of significance, we find that the transitions predicted with TD-CAM-B3LYP/AUG-cc-pVTZ are in pleasing agreement with the observed evidence (Table 1). Also the LCOAO results are consistent with the experimental evidence, even in the region of high wavenumbers (S3).

5. Conclusions

In this work, LD polarization data in the range $15,000$ – $58,000\text{ cm}^{-1}$ (667–172 nm) are provided for DSB dissolved and aligned in stretched PE, leading to the characterization of four main band systems A, B, C, and D with maxima at $27,600$, $41,000$, $49,800$, and close to $57,500\text{ cm}^{-1}$ (362, 244, 201, and 174 nm). The intense band A has been the object of several previous investigations, particularly in connection with studies of the photophysical properties of DSB [1–18]. The bands at higher wavenumbers seem to have attracted less attention. The analysis of the LD spectra is complicated by the low molecular symmetry of DSB, compared, for example, with the related chromophore BPEB (Scheme 1) [19]. According to the present results, bands A and C can be characterized as long axis-polarized, band D as predominantly short axis-polarized, while the features of band B are polarized at intermediate angles. We find that the theoretical transitions predicted with TD-CAM-B3LYP [39] and LCOAO [30,31] are in general agreement with the observed bands and their polarization directions. The ZINDO [28,29] and TD-LC ω PBE [36,37] procedures are less successful.

Author contributions

Duy Duc Nguyen conceived and designed the experiments, performed the experiments, analyzed the data, authored or reviewed drafts of the paper, approved the final draft. Nykola C. Jones and Søren V. Hoffmann conceived and designed the experiments, performed the experiments, contributed reagents/materials/analysis tools, authored or reviewed drafts of the paper, approved the final draft. Jens Spanget-Larsen conceived and designed the experiments, analyzed the data, contributed reagents/materials/analysis tools, prepared figures and/or tables, performed the computation work, authored or reviewed drafts of the paper,

approved the final draft.

Declaration of Competing Interest

The authors declare that they have no known competing financial interests or personal relationships that could have appeared to influence the work reported in this paper.

Data availability

Spectroscopic data are available from the UV-Vis⁺ Photochemistry Database (<https://science-softcon.de/spectra/>).

Acknowledgements

This investigation was supported by grants of beam time on the CD1 beamline at ISA. The stay of Nguyen Duc Duy at Roskilde University was enabled by a Ph.D. scholarship granted by the Vietnamese Ministry of Education and Training. The Danish International Development Agency (DANIDA) provided additional support via the Enhancement of Research Capacity (ENRECA) program. The authors are indebted to Eva M. Karlsen for technical assistance.

Appendix A. Supplementary material

Supplementary data to this article can be found online at <https://doi.org/10.1016/j.saa.2022.122019>.

References

- T. Damerou, M. Hennecke, Determination of orientational order parameters of uniaxial films with a commercial 90°-angle fluorescence spectrometer, *J. Chem. Phys.* 103 (1995) 6232–6240.
- H.-J. Egelhaaf, J. Gierschner, D. Oelkrug, Characterization of oriented oligo (phenylenevinylene) films and nano-aggregates by UV/Vis-absorption and fluorescence anisotropy, *Synth. Met.* 83 (1996) 221–226.
- H.-J. Egelhaaf, L. Lüer, A. Tompert, P. Bäuerle, K. Müllen, D. Oelkrug, Fluorescence anisotropy and rotational diffusion of polyene-like molecules in solution, *Synth. Met.* 115 (2000) 63–68.
- J. Gierschner, H.-G. Mack, L. Lüer, D. Oelkrug, Fluorescence and absorption spectra of oligophenylenevinylenes: vibronic coupling, band shapes, and solvatochromism, *J. Chem. Phys.* 116 (2002) 8596–8608.
- C.-J. Kim, Electronic properties and conformation analysis of π -conjugated distyryl benzene derivatives, *Bull. Korean Chem. Soc.* 23 (2002) 330–336.
- J. Gierschner, M. Ehni, H.-J. Egelhaaf, B. Milián Medina, D. Beljonne, H. Benmansour, G.C. Bazan, Solid state optical properties of linear polyconjugated molecules: π -stack contra herringbone, *J. Chem. Phys.* 123 (2005) 144914.
- H.-W. Wang, C. Chen, F.-C. Hsu, H.-C. Shieh, J.K. Wang, S.H. Lin, M. Hayashia, Theoretical studies of distyrylbenzene and its optical properties, *J. Chin. Chem. Soc.* 52 (2005) 665–675.
- C.C. Wu, E. Ehrenfreund, J.J. Gutierrez, J.P. Ferraris, Z.V. Vardeny, Apparent vibrational side bands in π -conjugated systems: the case of distyrylbenzene, *Phys. Rev. B* 71 (2005) 081201(R).
- C. Vijayakumar, V.K. Praveen, K.K. Kartha, A. Ajayaghosh, Excitation energy migration in oligo(p-phenylenevinylene) based organogels: structure-property relationship and FRET efficiency, *Phys. Chem. Chem. Phys.* 13 (2011) 4942–4949.
- J. Gierschner, S.Y. Park, Luminescent distyrylbenzenes: tailoring molecular structure and crystalline morphology, *J. Mater. Chem. C* 1 (2013) 5818–5832.
- J. Gierschner, L. Lüer, B. Milián-Medina, D. Oelkrug, H.-J. Egelhaaf, Highly emissive H-aggregates or aggregation-induced emission quenching? The photophysics of all-trans para-distyrylbenzene, *J. Phys. Chem. Lett.* 4 (2013) 2686–2697.
- B.J. Laughlin, T.L. Duniho, S.J. El Homsí, B.E. Levy, N. Deligonul, J.R. Gaffan, J.D. Protasiewicz, A.G. Tennyson, R.C. Smith, Comparison of 1,4-distyrylfluorene and 1,4-distyrylbenzene analogues: synthesis, structure, electrochemistry and photophysics, *Org. Biomol. Chem.* 11 (2013) 5425–5434.
- M. Wykes, S.K. Park, S. Bhattacharyya, S. Varghese, J.E. Kwon, D.R. Whang, I. Cho, R. Wannemacher, L. Lüer, S.Y. Park, J. Gierschner, Excited state features and dynamics in a distyrylbenzene-based mixed stack donor–acceptor cocrystal with luminescent charge transfer characteristics, *J. Phys. Chem. Lett.* 6 (18) (2015) 3682–3687.
- E.F. Oliveira, J. Shi, F.C. Lavarda, L. Lüer, B. Milián-Medina, J. Gierschner, Excited state absorption spectra of dissolved and aggregated distyrylbenzene: a TD-DFT state and vibronic analysis, *J. Chem. Phys.* 147 (2017), 034903.
- S.E. Estrada-Flórez, F.S. Moncada, A.E. Lanterna, C.A. Sierra, J.C. Scaiano, Spectroscopic and time-dependent DFT study of the photophysical properties of substituted 1,4-distyrylbenzenes, *J. Phys. Chem. A* 123 (30) (2019) 6496–6505.
- X. Sheng, H. Zhu, K. Yin, J. Chen, J. Wang, C. Wang, J. Shao, F. Chen, Excited-state absorption by linear response time-dependent density functional theory, *J. Phys. Chem. C* 124 (2020) 4693–4700.
- J.C. Roldao, E.F. Oliveira, B. Milián-Medina, J. Gierschner, D. Roca-Sanjuán, Quantum-chemistry study of the ground and excited state absorption of distyrylbenzene: multi vs single reference methods, *J. Chem. Phys.* 156 (2022), 044102.
- J.C. Roldao, E.F. Oliveira, B. Milián-Medina, J. Gierschner, D. Roca-Sanjuán, Accurate calculation of excited-state absorption for small-to-medium-sized conjugated oligomers: multiconfigurational treatment vs quadratic response TD-DFT, *J. Chem. Theory Comput.* 18 (2022) 5448–5449.
- D.D. Nguyen, N.C. Jones, S.V. Hoffmann, S.H. Andersen, P.W. Thulstrup, J. Spanget-Larsen, Electronic states of 1,4-bis(phenylethynyl)benzene: a synchrotron radiation linear dichroism investigation, *Chem. Phys.* 392 (2012) 130–135.
- J. Michl, E.W. Thulstrup, Spectroscopy with Polarized Light. Solute Alignment by Photoselection, in *Liquid Crystals, Polymers and Membranes*, VCH-Wiley, Deerfield Beach, FL, 1986, 1995.
- E.W. Thulstrup, J. Michl, *Elementary Polarization Spectroscopy*, Wiley-VCH, New York, Weinheim, 1989.
- F. Madsen, I. Terpager, K. Olskær, J. Spanget-Larsen, Ultraviolet-visible and infrared linear dichroism spectroscopy of 1,8-dihydroxy-9,10-anthraquinone aligned in stretched polyethylene, *Chem. Phys.* 165 (2-3) (1992) 351–360.
- A. Rodger, B. Nordén, *Circular Dichroism and Linear Dichroism*, Oxford University Press, UK, 1997.
- B. Nordén, A. Rodger, T. Dafforn, *Linear Dichroism and Circular Dichroism: A Textbook on Polarized-light Spectroscopy*, RCS Publishing, Cambridge, UK, 2010.
- E.W. Thulstrup, J. Waluk, J. Spanget-Larsen, Electronic spectroscopy: linear dichroism, applications, in: J.C. Lindon, G.E. Tranter, D.W. Koppenaal (Eds.), *Encyclopedia of Spectroscopy and Spectrometry*, third edition, Academic Press, Oxford, UK, 2017, pp. 595–600, doi: 10.1016/B978-0-12-803224-4.00190-4.
- A.J. Miles, S.V. Hoffmann, Y. Tao, R.W. Janes, B.A. Wallace, Synchrotron radiation circular dichroism (SRCD) spectroscopy: new beamlines and new applications in biology, *Spectroscopy* 21 (2007) 245–255.
- A.J. Miles, R.W. Janes, A. Brown, D.T. Clarke, J.C. Sutherland, Y. Tao, B. A. Wallace, S.V. Hoffmann, Light flux density threshold at which protein denaturation is induced by synchrotron radiation circular dichroism beamlines, *J. Synchrotron Rad.* 15 (4) (2008) 420–422.
- J. Ridley, M. Zerner, An intermediate neglect of differential overlap technique for spectroscopy: pyrrole and the azines, *Theoret. Chem. Acc.* 32 (2) (1973) 111–134.
- M.C. Zerner, in: K.B. Lipkowitz, D.B. Boyd (Eds.), *Reviews of Computational Chemistry, Vol. 2*, VCH Publishing, New York, 1991, pp. 313–366.
- J. Spanget-Larsen, The alternating hydrocarbon pairing theorem and all-valence electrons theory. An approximate LCOAO theory for the electronic absorption and MCD spectra of conjugated organic compounds. 1, *Croat. Chem. Acta.* 59 (1986) 711–717.
- J. Spanget-Larsen, The alternant hydrocarbon pairing theorem and all-valence electrons theory. An approximate LCOAO theory for the electronic absorption and MCD spectra of conjugated organic compounds. 2, *Theoret. Chem. Acc.* 98 (1997) 137–153.
- S. Grimme, Calculation of the electronic spectra of large molecules, *Rev. Comp. Chem.* 20 (2004) 153–218.
- M.E. Casida, Review: time-dependent density-functional theory for molecules and molecular solids, *J. Mol. Struct. Theochem.* 914 (2009) 3–18.
- C. Adamo, D. Jacquemin, The calculations of excited-state properties with time-dependent density functional theory, *Chem. Soc. Rev.* 42 (3) (2013) 845–856.
- J.B. Foresman, A.E. Frisch, *Exploring Chemistry with Electronic Structure Methods*, third edition, Gaussian Inc, Wallingford, CT, 2015.
- Y. Tawada, T. Tsuneda, S. Yanagisawa, T. Yanai, K. Hirao, A long-range-corrected time-dependent density functional theory, *J. Chem. Phys.* 120 (2004) 8425.
- O.A. Vydrov, J. Heyd, A.V. Kruckov, G.E. Scuseria, Importance of short-range versus long-range Hartree-Fock exchange for the performance of hybrid density functionals, *J. Chem. Phys.* 125 (7) (2006) 074106.
- J.-D. Chai, M. Head-Gordon, Long-range corrected hybrid density functionals with damped atom-atom dispersion corrections, *Phys. Chem. Chem. Phys.* 10 (2008) 6615–6620.
- T. Yanai, D. Tew, N.A. Handy, New hybrid exchange-correlation functional using the Coulomb-attenuating method (CAM-B3LYP), *Chem. Phys. Lett.* 393 (2004) 51–57.
- L.Y. Malkes, T.P. Boronenko, Ultraviolet absorption spectra of ω -triaryl-substituted 1,2,4-trivinylbenzenes, *J. Appl. Spectrosc.* 21 (1) (1974) 976–979.
- UV/Vis⁺ photochemistry database, <https://science-softcon.de/spectra/aromatics/arocom1.php?q=1,4-distyrylbenzene#1608-41-9> (Accessed 27 June 2022).
- M.J. Frisch, G.W. Trucks, H.B. Schlegel, G.E. Scuseria, M.A. Robb, J.R. Cheeseman, G. Scalmani, V. Barone, G.A. Petersson, H. Nakatsuji, X. Li, M. Caricato, A.V. Marenich, J. Bloino, B.G. Janesko, R. Gomperts, B. Mennucci, H.P. Hratchian, J.V. Ortiz, A.F. Izmaylov, J.L. Sonnenberg, D. Williams-Young, F. Ding, F. Lipparini, F. Egidi, J. Goings, B. Peng, A. Petrone, T. Henderson, D. Ranasinghe, V.G. Zakrzewski, J. Gao, N. Rega, G. Zheng, W. Liang, M. Hada, M. Ehara, K. Toyota, R. Fukuda, J. Hasegawa, M. Ishida, T. Nakajima, Y. Honda, O. Kitao, H. Nakai, T. Vreven, K. Throssell, J.A. Montgomery, Jr., J.E. Peralta, F. Ogliaro, M.J. Bearpark, J. J. Heyd, E.N. Brothers, K.N. Kudin, V.N. Staroverov, T.A. Keith, R. Kobayashi, J. Normand, K. Raghavachari, A.P. Rendell, J.C. Burant, S.S. Iyengar, J. Tomasi, M. Cossi, J.M. Millam, M. Klene, C. Adamo, R. Cammi, J. W. Ochterski, R.L. Martin, K.

- Morokuma, O. Farkas, J.B. Foresman, D.J. Fox, Gaussian 16, Revision A.03, Gaussian, Inc., Wallingford, CT, 2016.
- [43] J. Spanget-Larsen, LCOAO Computer Program: Fortran source code with sample input and output, ResearchGate (2014). 10.13140/2.1.3455.6482.
- [44] T.H. Dunning, Gaussian basis sets for use in correlated molecular calculations. I. The atoms boron through neon and hydrogen, *J. Chem. Phys.* 90 (2) (1989) 1007–1023.
- [45] R.A. Kendall, T.H. Dunning, R.J. Harrison, Electron affinities of the first-row atoms revisited. Systematic basis sets and wave functions, *J. Chem. Phys.* 96 (9) (1992) 6796–6806.
- [46] S. Grimme, S. Ehrlich, L. Goerigk, Effect of the damping function in dispersion corrected density functional theory, *J. Comp. Chem.* 32 (7) (2011) 1456–1465.
- [47] S. Miertuš, E. Scrocco, J. Tomasi, Electrostatic interaction of a solute with a continuum. A direct utilization of AB initio molecular potentials for the prevision of solvent effects, *Chem. Phys.* 55 (1) (1981) 117–129.
- [48] J. Tomasi, M. Persico, Molecular interactions in solution: an overview of methods based on continuous distributions of the solvent, *Chem. Rev.* 94 (1994) 2027–2094.
- [49] C.J. Cramer, D.G. Truhlar, Implicit solvation models: equilibria, structure, spectra, and dynamics, *Chem. Rev.* 99 (1999) 2161–2200.
- [50] G. Scalmani, M.J. Frisch, Continuous surface charge polarizable continuum models of solvation. I. General formalism, *J. Chem. Phys.* 132 (2010), 114110.
- [51] J. Michl, Magnetic circular dichroism of aromatic molecules, *Tetrahedron* 40 (1984) 3845–3934.
- [52] A.D. Becke, Density-functional thermochemistry. III. The role of exact exchange, *J. Chem. Phys.* 98 (1993) 5648–5652.
- [53] C. Lee, W. Yang, R.G. Parr, Development of the Colle-Salvetti correlation-energy formula into a functional of the electron density, *Phys. Rev. B: Condens. Matter Mater. Phys.* 37 (2) (1988) 785–789.
- [54] R. Dennington, T.A. Keith, J.M. Millam, GaussView, Version 6.0.16, Semichem Inc., Shawnee Mission, Kansas, USA, 2016.
- [55] M. Levitus, K. Schmieder, H. Ricks, K.D. Shimizu, U.H.F. Bunz, M.A. Garcia-Garibay, Steps to demarcate the effects of chromophore aggregation and planarization in poly(phenyleneethynylene)s. 1. Rotationally interrupted conjugation in the excited states of 1,4-bis(phenylethynyl)benzene, *J. Am. Chem. Soc.* 123 (18) (2001) 4259–4265.
- [56] M. Levitus, M.A. Garcia-Garibay, Polarized electronic spectroscopy and photophysical properties of 9,10-bis(phenylethynyl)anthracene, *J. Phys. Chem. A* 104 (38) (2000) 8632–8637.
- [57] P.W. Thulstrup, N.C. Jones, S.V. Hoffmann, J. Spanget-Larsen, Electronic states of the fluorophore 9,10-bis(phenylethynyl)anthracene (BPEA). A synchrotron radiation linear dichroism investigation, *Chem. Phys. Lett.* 559 (2013) 35–40.